Steel and Composite Structures, Vol. 2, No. 5 (2002) 397-410
DOI: http://dx.doi.org/10.12989/scs.2002.2.5.397

Structural assessment of cold-formed composite structures

S.A.L. de Andrade†

Civil Engineering Department, PUC, Rio de Janeiro, Brazil, Structural Engineering Department, UERJ, Rio de Janeiro, Brazil

P.C.G. da S. Vellasco†

Structural Engineering Department, UERJ, Rio de Janeiro, Brazil

A.J.R. Mergulhão‡

Civil Engineering Department, UFOP, Minas Gerais, Brazil

(Received April 11, 2002, Accepted September 23, 2002)

Abstract. The main aim of the present paper is to present the results of a full-scale experimental investigation to study the structural behaviour of composite steel beams. The composite beam was made of cold-formed steel section shapes filled with reinforced concrete. First a comprehensive description of the experimental results in terms of: deflections, deformations, slippage and stress levels on critical steps of the load path is presented. The experimental results were then compared to theoretical values obtained by the use of an analytical model based on ultimate limit state stress blocks. Finally, a practical application of the use of this structural solution is depicted.

Key words: composite construction; cold-formed structures; experimental analysis; composite structural design; structural behaviour; cold-formed composite structures.

1. Introduction

The first investigations on the behaviour of steel structures filled with reinforced concrete took place in Germany in the 70's, (Jungbluth and Gradwohl 1985, Jungbluth 1986, Jungbluth and Gradwohl 1998, Berner 1988). The main objective of these investigations was to evaluate composite structural systems strength when exposed to high temperatures (fire conditions). A structural system made of steel profiles (laminated or welded) with the region between the flanges filled with reinforced concrete was proposed and developed, Fig. 1. In this system, the interaction between the reinforced concrete and the steel profile was guaranteed by shear connectors or stirrups welded to the beam web.

Lehtola (1992) extended this research to cover the composite cold-formed structures at the Civil Engineering Department of PUC-RIO, developing a series of computer programs for composite cold-

†Associate Professor
‡Senior Lecturer

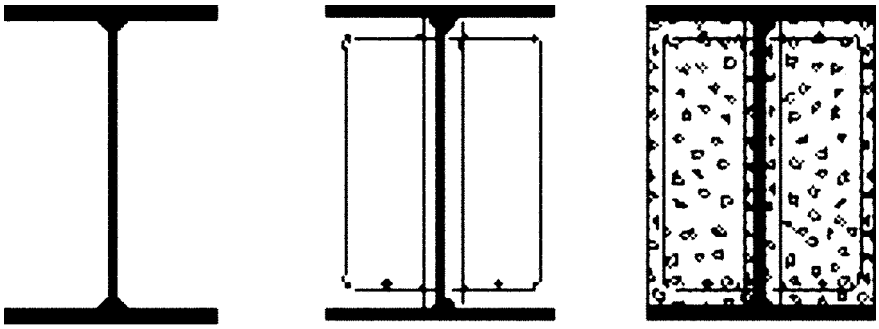

Fig. 1 (a) Welded I-shape; (b) Welded I-shape with bars and stirrups; (c) Welded I-shape filed with reinforced concrete

formed strength evaluation. The main objective of his work was to create graphical tools, to help on the composite cold-formed structural design. Although its results were promising, the simplifications hypothesis used in the SCCSD program (Steel-Concrete Composite Structures Design) needed to be corroborated by experiments.

Up to the present moment no experiments were available on the structural response of composite cold-formed structures. This fact motivated the development of an experimental program to calibrate the assumed hypothesis. A full-scale experimental program was then conducted at the Structural Laboratory of the Civil Engineering Department, PUC-RIO, where two simply supported beams were tested. The beams were assembled and tested with a 12 metre span and were subjected to bending. A comparison of the tests results with predicted values of the SCCSD program (Lehtola 1992) was also performed.

2. Theoretical behaviour

The computer programs (WSST, CFSST, SCCSD) used to obtain the theoretical results were developed by Lehtola (1992), Andrade (1995). The program CFSST (Cold-Formed Steel Shape Tool) is a design tool to create the shape of cold-formed cross sections. This program allows the user to shape and obtain the geometric properties of the desired cross-section. The cold-formed shaping operation through CFSST program is performed by a series of mechanical foldings and adjustments to the steel plate till the desired configuration of the cold-formed cross-section is obtained.

The WSST program (Welded Steel Shape Tool) is a steel cross-section assembler. The elements of the cross section are composed of cold-formed plates. The WSST allows the combination or connection of geometric entities without allowing an overlap of the parts being connected. The cross section assembly, through WSST, consists of successive combinations of cold-formed entities previously created.

The SCCSD program (Steel-Concrete Composite Structures Design) was developed to evaluate the structural strength of composite cold-formed sections, Figs. 2 and 3. It also evaluates the structures behaviour under fire conditions. This program offers the user, through a graphical interface, the ability to build up a composite section and allows modifications of the physical and geometrical characteristics

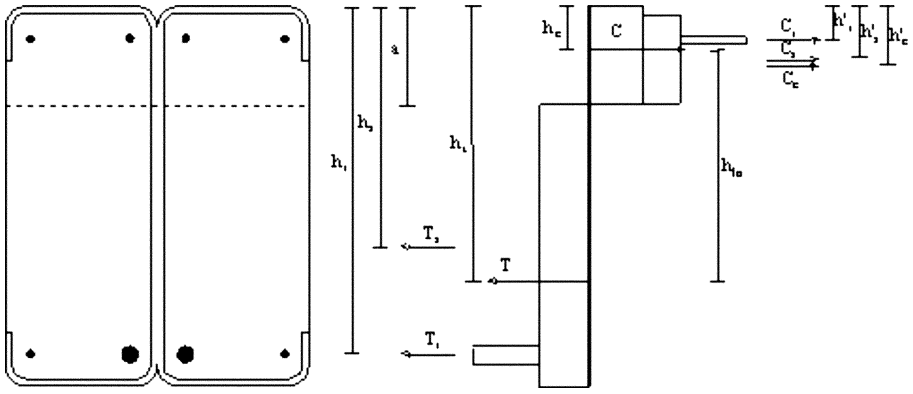

Fig. 2 Ultimate limit state stress block diagrams

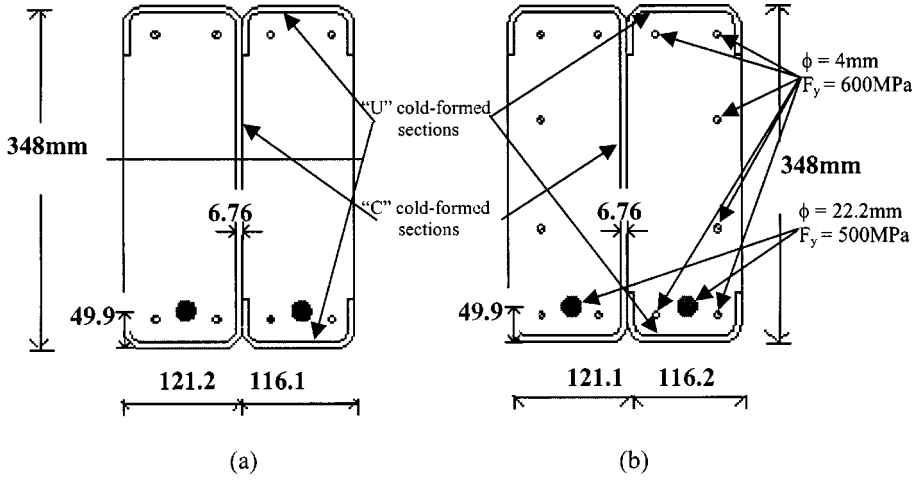

Fig. 3 Cross-section shape of the first and second tested beams

of the cross-section elements.

The SCCSD program was used to evaluate the resistance of a composite cold-formed beam filled with reinforced concrete. The flexural resistance of the composite section, Eqs. (1) to (3), is determined through equilibrium on the stress block diagram shown in Fig. 2. The calculated flexural strength is based on the steel versus concrete full interaction hypothesis. The program can also evaluate the increase in bending resistance provided by the use of a concrete slab.

$$M_U = C_R(h_t - h_r') + C_S(h_t - h_S') + C_c(h_t - h_c') \tag{1}$$

where:

$$C_R = f_{yr}A_{rc}, \quad C_S = f_yA_{sc}, \quad C_c = f_{cr}A_{cr}, \quad T_R = f_{yr}A_{rt}, \quad T_S = f_yA_{st} \tag{2}$$

$$C = C_R + C_S + C_c, \quad T = T_R + T_S, \quad C = T \tag{3}$$

The total beam deflections evaluated by Eqs. (4) to (6) considers the structure self-weight, Δ_{PL}, the

live load parcel Δ_{LL} and the shrinkage and creep effects Δ_{shrink} and Δ_{creep}, based on Chien *et al.* (1984):

$$\Delta=\Delta_{SW}+\Delta_{shrink}+\Delta_{creep}+\Delta_{LL} \tag{4}$$

where:

$$\Delta_{creep}=\frac{5W_{LT}L^3}{384E}\left(\frac{1}{I_r}+\frac{1}{I_T}\right),\quad \Delta_{SW}=\frac{5W_{SW}L^3}{384EI_s},\quad \Delta_{shrink}=\frac{0.0002A_{rc}L^2(a-h_c)}{8nI_T},\quad \Delta_{LL}=\frac{5W_{LL}L^3}{384EI_e} \tag{5}$$

$$I_e=I_s+0.85(I_T-I_s),\quad n=E/E_c,\quad E_c=0.043\gamma_{cr}^{1.5}\sqrt{f_{cr}} \tag{6}$$

3. Experimental results

This section presents the experimental results in terms of: deflections, deformations and stress distributions for the two tested beams, Fig. 3 (Mergulhão 1994). The beams were tested with the aid of four hydraulics jacks, Fig. 4, to simulate internal forces equivalent to a uniform load distribution. To ensure the correct boundary conditions between the jacks and the beam's top flange an arrangement that included a hinge, a load cell and cylindrical rollers was used, Fig. 5.

3.1. The first test

Three pre-loads were performed to adjust the hydraulics jacks, supports and instrumentation gadgets used to measure loads, deformations, deflections and slippage, Table 1.

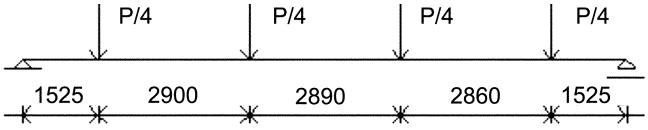

Fig. 4 Load configuration scheme (units in mm)

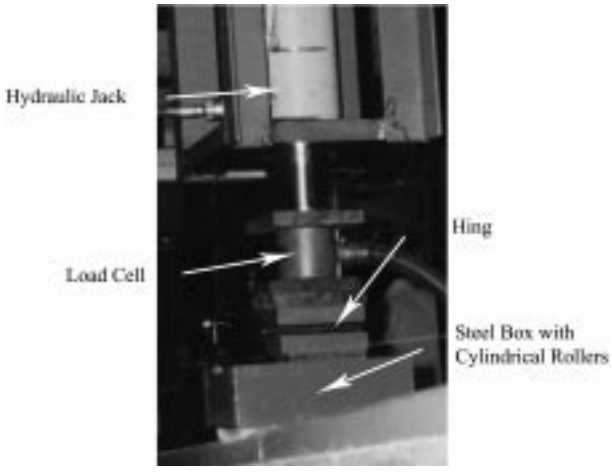

Fig. 5 Load application point detail

Table 1 First test results

Test	Maximum Load (kN)	Maximum Deflection (mm)	Residual Deflection (mm)
First Pre-Load	57.6	37.8	3.7
Second Pre-Load	100.8	69.7	5.3
Third Pre-Load	139.2	99.5	20.3
Final Test	240.0	225.1	–

Fig. 6 Experiments general layout scheme

The first pre-load was conducted when the concrete had cured 53 days. The maximum load corresponded to 57.6 kN with a maximum deflection of 37.8 mm measured at centre span. The beam remained with a residual deflection of 3.7 mm when unloaded. In the second pre-load, made on the same day, the structure was loaded up to 100.8 kN. The maximum deflection obtained at the centre span was 69.7 mm and the residual deflection was 5.3 mm. In the third pre-load, still made on the same day, the structure was loaded up to 139.2 kN, with a maximum deflection of 99.5 mm and a total residual deflection of 20.3 mm, Fig. 6.

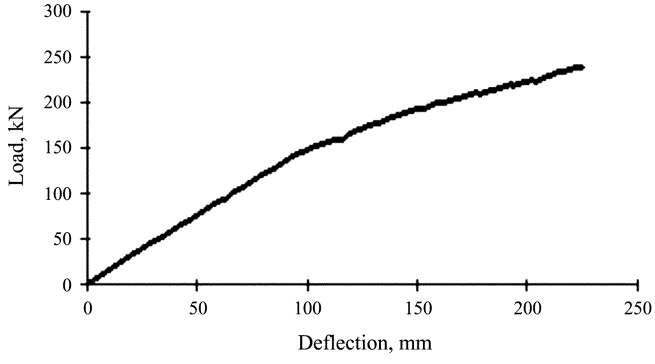

Fig. 7 First test load versus central section vertical displacement

Fig. 8 First test bottom flange weld rupture

The deflections were measured at the beam's quarter span through three LVDTS (Linear Variable Differential Transducers) located at the top flange. The deflections at centre span are presented in Fig. 7 up to the beam's collapse. The collapse mode reported was related to a bottom flange weld rupture close to centre span. The final recorded load was 240.2 kN and the maximum deflections corresponded to 225.1 mm, larger than the maximum allowable deflection of span/360, i.e., 32.5 mm, as shown in Fig. 8.

Fig. 9(a) presents the beam's load vs. deformations behaviour, measured by two strain gauges located at the bottom flange, 200 mm far from the centre of the beam. A non-linear behaviour begins to appear for load values greater than 120 kN. The onset of steel yielding deformations corresponded to load values of 176.8 kN and 187.5 kN, respectively with a 6% difference. At the peak load, the deformations reached 1.6 and 1.9 times the yield deformation, ε_y.

A load versus normalised deformations graph for two reinforcement bars located near the tension part of the steel section are depicted in Fig. 9(b). The deformations were obtained by two strain gauges positioned at the bottom face of each bar, 200 mm far from the central section of the beam. The curves are very similar showing a symmetric behaviour. The yield stress of the steel bar was reached at a load value of 253.0 kN.

The stress distribution along the beam's height, Fig. 10, was obtained by means of deformation values measured through strain gauges at the top and bottom flanges of the cold-formed steel profile and at the reinforcement bars. The analysed section was located 200 mm from the centre of the beam.

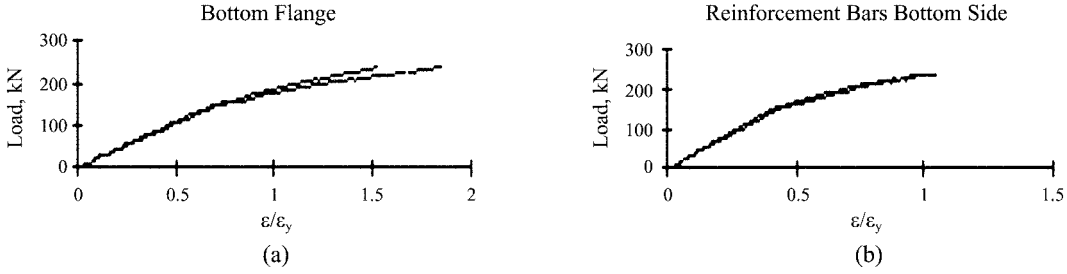

Fig. 9 First test load versus normalised deformation

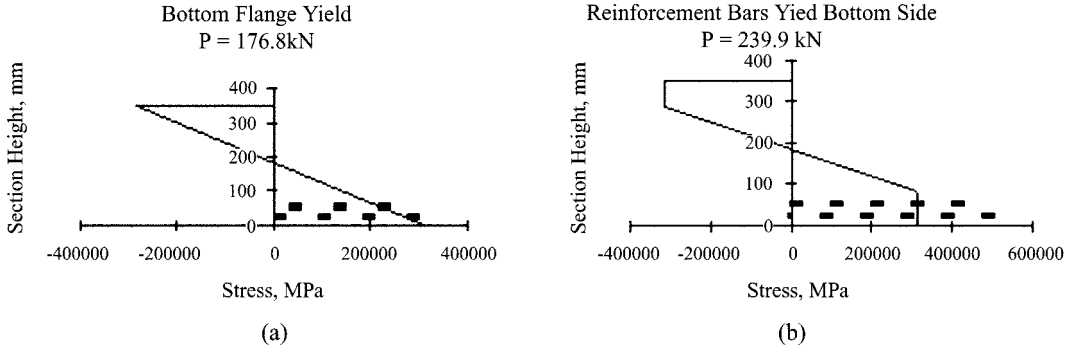

Fig. 10 Stress distribution at the cross-section of the first test

The initial yield of the cold-formed bottom flange was obtained at a load value corresponding to 176.8 kN, Fig. 10(a). At this load level the stress in top flange corresponded to 280.9 MPa, while the top and bottom faces of the reinforcement bars, represented by the dotted lines, reached 239.2 MPa and 298.7 MPa, respectively.

When the load reached 233.9 kN the bottom reinforcement bars begin to yield presenting a stress of 499.9 MPa, Fig. 10(b). At the same load level it was possible to notice that a great part of the steel cross section was yielded with 315.1 MPa while the top reinforcement bars, represented by the dotted lines, reached 424.6 MPa. No slippage was measured in the steel concrete interface despite the fact that no shear connectors were used in this test.

3.2. The second test

When the concrete reached 44 days, a single pre-load was conducted. This corresponded to a load of 28 kN and led to a maximum vertical central displacement of 15.2 mm. When the unloading phase was finished the structure presented a residual deflection of 1.9 mm, Table 2.

The final test, made on the same day of the preload test, took seventeen hours to be carried out. When the load level corresponded to 210 kN, the maximum central jack's course was reached leading to the structure to be anchored at the reaction slab of the laboratory. When this task was completed the jacks were moved down and the test proceeded normally. Fig. 11 shows a deformed configuration of the second beam during the loading phase. When the applied load value was approaching 284.3 kN, a weld rupture at the single cold-formed *U* of the bottom flange, at centre span, was noticed leading to the structure's collapse. A maximum load of 284.6 kN was recorded shortly after the weld rupture.

Fig. 12 presents the load versus vertical displacement curve measured by a LVDT (Linear Variable Differential Transducers) installed at centre span. A non-linear behaviour was noticed for load values

Table 2 Second test results

Test	Maximum Load (kN)	Maximum Deflection (mm)	Residual Deflection (mm)
Pre-Load	28.0	15.2	1.9
Final Test	284.6	452.6	–

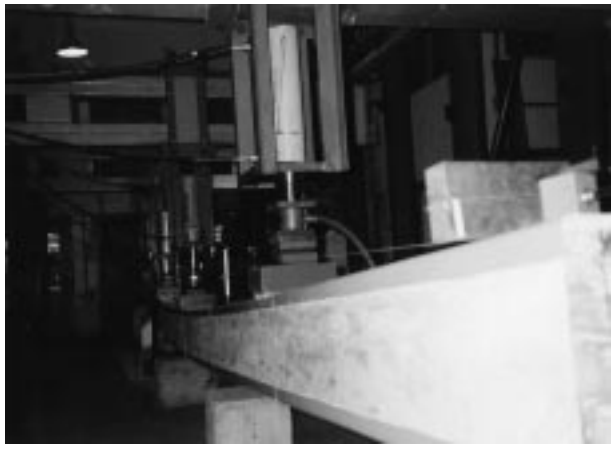

Fig. 11 Second test deformed configuration under loading

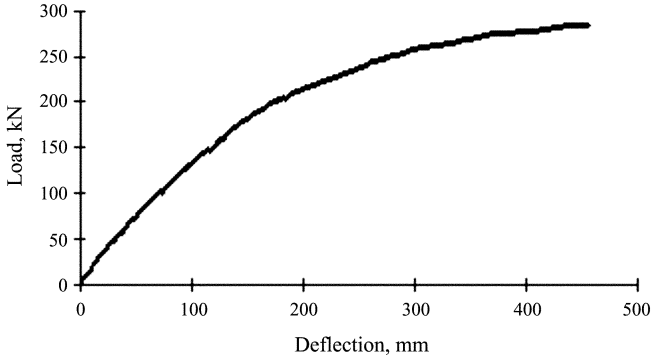

Fig. 12 Second test load versus central section vertical displacement

greater than 122.2 kN. From this load up, which corresponded to a deflection value of 89.9 mm, the deflections increased considerably. The maximum recorded load was 284.6 kN, very close to the theoretical load of 284.3 kN. The maximum recorded deflection was 452.6 mm, which is well over the serviceability limit of span over 360.

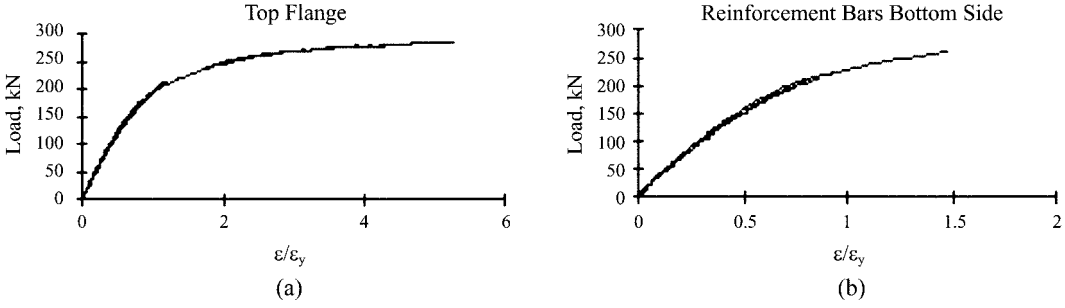

Fig. 13 Second test load versus normalized deformation

Fig. 13(a) presents two deformation's curves for points located at the top flange of the cold-formed section, recorded by two strain-gauges 150 mm from the beam's centre. The curves are almost identical, presenting a linear behaviour for load values less than 109 kN. Yield deformation occurred for load values corresponding to 196.4 kN and 193.5 kN. When the applied loading reached its maximum value, the deformations were five times the yield values.

Fig. 13(b) shows the applied load versus deformations of the two reinforcement bars. Deformations were obtained by two strain gauges located at their bottom side, 150 mm far from the beam's centre. The graphics are almost identical, and yielding occurred at a load value of 220 kN.

Figs. 14 and 15 illustrate the cross-section stress distribution at a section 150 mm far from the beam's centre. The stress values were obtained by recorded deformations at linear strain gauges located on the bottom and top of the cold-formed flanges and reinforcement bars. Rosettes strain gauges were used in the web. When the applied load was 170.8 kN, a yield deformation began at the bottom flange of the cold-formed section, Fig. 14(a). At this load level the stress values recorded corresponded to: 24.4 MPa in the web, 269.9 MPa at the bottom reinforcement bars, represented by the dotted lines, and 251.1 MPa at top flange of the cold-formed section. Top flange yield occurred at a 196.4 kN, Fig. 14(b). The stress values at this load level corresponded to: 33.4 MPa in the web and 342.6 MPa at the bottom reinforcement bar.

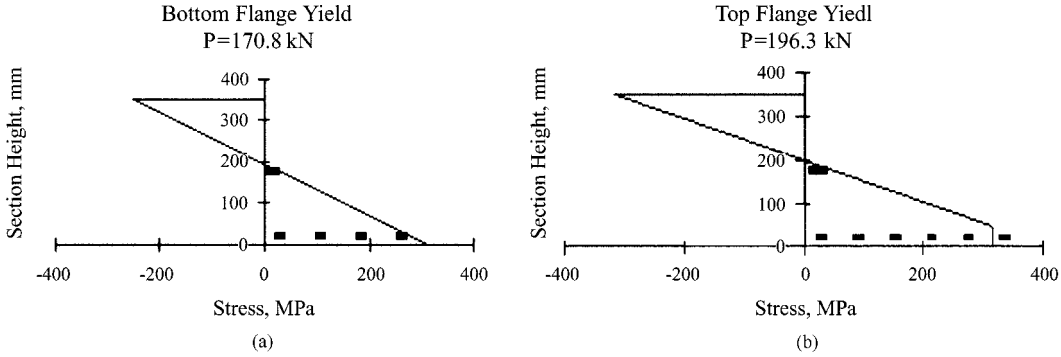

Fig. 14 Stress distribution at the cross-section of the second test

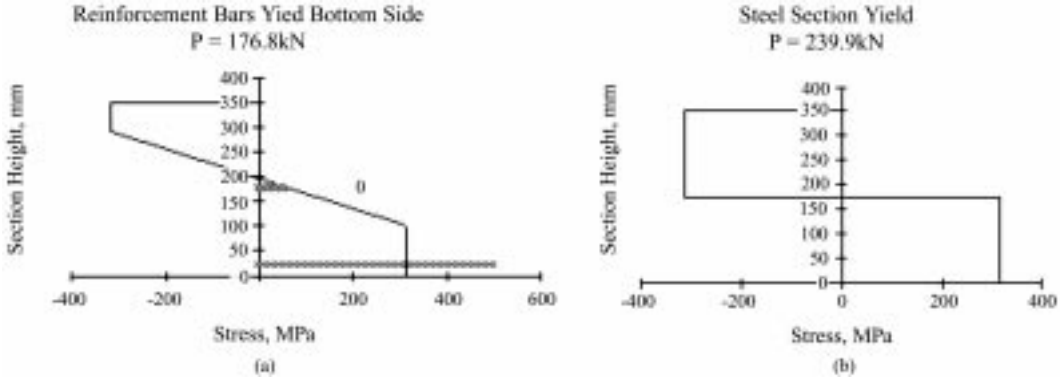

Fig. 15 Stress distribution at the cross-section of the second test

Fig. 15(a) presents most of the steel section plastification at a load level of 229.2 kN. At this load level the web and stress reinforcement bars, represented by the shadow lines, corresponded to 52.9 MPa, and 499.9 MPa. When the load reached 278.9 kN plastification at the web middle height occurred, Fig. 15(b). Once again no steel to concrete slip was measured despite the fact that no shear connectors were used in this test.

4. Theoretical results

A comparison is presented between the theoretical and experimental results for the ultimate bending resistance and deflections (Mergulhão 1994). The ultimate resistance was determined through SCCSD program (Steel-Concrete Composite Structure Design), based on Eqs. (1) to (3) (Lehtola 1992). Procedures presented by Chien *et al.* (1984), Eqs. (4) to (6), were used to calculate the deflection. Permanent and variable loads, long-term deformations and concrete shrinkage effects were considered. Nominal values of the actions were used and the maximum deflection recommended value used corresponded to 1/360 of the beam span (Brazilian Code 1986).

The cross-section presented in Fig. 3(a) was used to evaluate the design strength of the first beam. The average measured mechanical properties of the concrete, cold-formed and reinforcement bars presented, respectively, the following values: 21.9 MPa, 314.9 MPa and 612.6 MPa. The diameters of the reinforcement bars used to model the problem were 4 mm and 22.2 mm respectively. Four millimetre stirrup bars 200 mm spaced were used to ensure the position the longitudinal reinforcement bars inside the steel profile as can be seen in Fig. 16. The first test moment capacity, evaluated through the SCCSD program (Lehtola 1992), was 424.8 kNm corresponding to an ultimate load of 282.8 kN. The maximum experimental load was 240 kN leading to a 17.8% difference, Table 3.

The second beam used two longitudinal reinforced bars with 4mm diameter located at each concrete

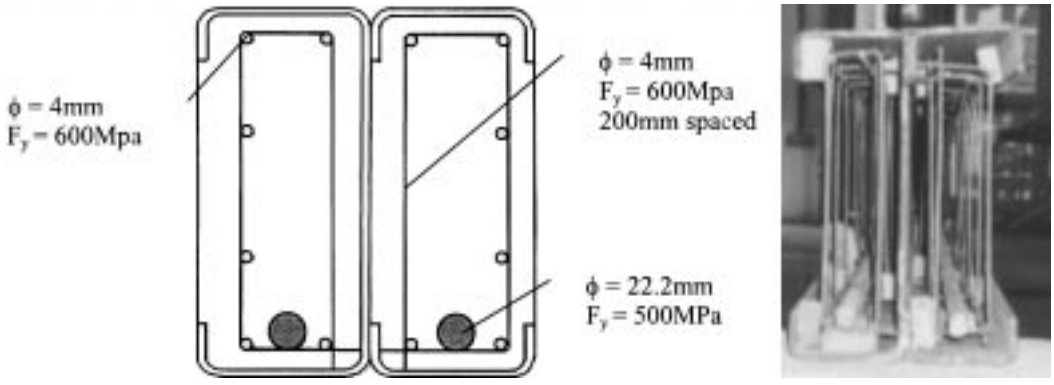

Fig. 16 Cross-section reinforcement bars detail used on the second tested beam

Table 3 Ultimate bending resistance comparison

Test	Theoretical Load (kN)	Experimental Load (kN)	Difference (%)
First Test	282.8	240.0	17.8
Second Test	284.3	284.6	0.1

Table 4 Theoretical and experimental total deflections (units in mm)

Vertical Deflections	First Test	Second Test
Experimental Deflections	131.8	143.1
Theoretical Deflections	120.0	125.6
% Difference	8.9%	13.7%

face, 120 mm apart to prevent the appearance of cracks. Similar four millimetre stirrup bars 200 mm spaced were used to ensure the position of the longitudinal reinforcement bars inside the steel profile as can be seen in Fig. 16. The weld joint located 4500 mm far from the two extremities of the beam, were strengthened with an external cold-formed *U* section, with 6.3 mm thickness and 300 mm length positioned surrounding the beam bottom flange as a sleeve plate.

The cross-section presented in Fig. 3(b) was used to evaluate the design strength of the second beam. The average mechanical properties of the concrete, cold-formed section and reinforcement bars were: 21.6 MPa, 314.9 MPa and 612.6 MPa, respectively. The reinforcement bars diameters used in this beam were 4 mm and 22.2 mm. The second beam moment capacity, evaluated through SCCSD program

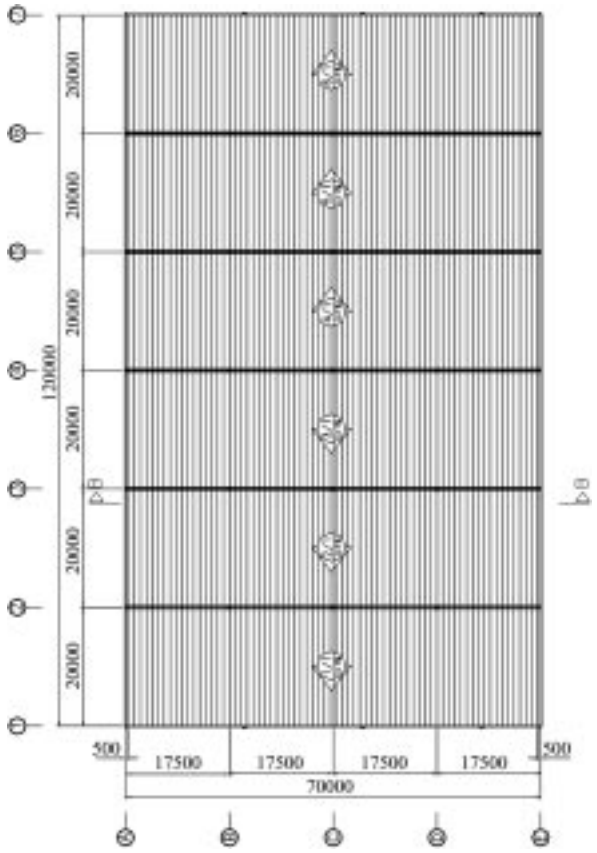

Fig. 17 Typical warehouse building

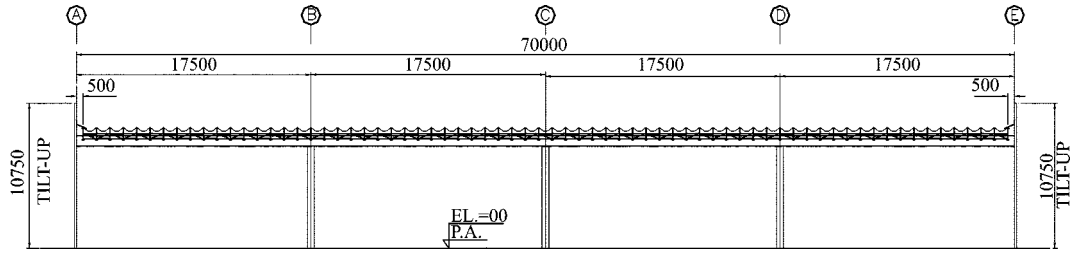

Fig. 18 Typical warehouse building cross-section

(Lehtola 1992) was 427.1 kNm corresponding to an ultimate load of 284.3 kN. The maximum experimental load was 284.6 kN leading to a 0.1% difference, Table 3.

Experimental deflections were evaluated at a loading level corresponding to the adopted values for permanent and variable loads. This strategy was used to make possible a comparison of theoretical and experimental deflections. The theoretical and experimental total deflections for the first and second tests are presented on Table 4. The first beam spanned 11700 mm, and was subjected to 25.1 kN self-weight and 150.8 kN live load leading to an experimental deflection of 131.8 mm. The second beam was subjected to 26.9 kN self-weight and 149.9 kN live load leading to an experimental deflection of 143.1 mm. These values are very close to the theoretical deflections. They corresponded to: 120 mm and 125.6 mm, for the first and second beams, and produced a 8.9% and 13.7% difference, respectively.

5. Practical application

A flat-roofed warehouse building, widely used in tilt-up construction, is depicted to demonstrate the applicability of the investigated type of composite beams. The building dimensions are 70m wide and 120m long, (Figs. 17 and 18). The building length is divided into six 20m equal spans. The open-web-steel-joists OWSJ, also spanning 20m, are supported along the axis 2, 3, 4, 5 and 6 by portal frames with 17.5m span. All outside walls are made of tilt-up panels with a 150 mm thickness. The building clear depth is 8m. The joists and roof permanent nominal loads are 0.25 kN/m^2, the imposed load is 0.15 kN/m^2 and the adopted uplift wind load is 0.60 kN/m^2.

In an all-steel design the supporting beam should have at least 700 mm depth requiring an extensive number of braces to prevent lateral torsional buckling. The proposed composite beam, possessing only 350 mm depth, can be used satisfactory in this project without the need of any bracing system. The use of a 75 mm camber in the beam would result in a total vertical deflection of 56 mm, (i.e., span over 312) attending all the serviceability checks.

6. Conclusions

Two full-size experiments were performed and compared with analytical results. The weld rupture present in the first test happened when the applied load value was equal to 85% of the ultimate load obtained by the program. On the other hand, the second test composite cold-formed section was fully

plastified at a load level corresponding to 98% of the ultimate load calculated by the program. These statements led to the conclusion that the difference between calculated values through theoretical procedure and experiments was smaller than 15% for all studied cases. No concrete failure or extensive cracking occurred in the tests.

A linear relationship between load and the deflection was obtained for the first beam up to 141.3 kN (approximately 59% of the ultimate load) with a 95.5 mm correspondent deflection. The test deflection at service condition was 131.8 mm. This value is very close to a theoretical deflection of 120 mm. The second beam, presented a linear behaviour, up to a load value of 122.2 kN (approximately 43% of the ultimate load) with an associated 89.9 mm of deflection. The test deflection was 143.1 mm, which is also very close to the theoretical deflections of 125.6 mm. The maximum difference in terms of deflections was 13.7%. The measured deflections would have been more accurate if long-term and shrinkage effects were considered.

The use of two back-to-back cold-formed channel sections instead of the current layout would have minimized the welding distortion problems found in the fabrication phase. The presence of the second web would also increase the composite section shear and fire resistances due to the second web extra thickness.

The presence of the reinforced concrete increased the inertia of the beam making the structure stiffer, and consequently leading to smaller deflections than a non-composite solution.

The theoretical and test values for the deflections were higher than the maximum Brazilian Code limits (1986). With this constraint in mind it is possible to calculate back the maximum allowable span for the tested cold-formed cross-section. With adopted permanent and live load used in multi-storey buildings this section could be used on beams up to 7.5 meters.

The tests presented no slippage in the steel concrete interface confirming that shear connectors welded to the steel section web, generally used in rolled and WWF steel beams, were not necessary for the tested cold-formed sections. This was mainly due to the extra bonding resistance provided by the three-dimensional state of stress generated in the confined concrete.

References

ABNT-NBR 8800/86; (1986), *Steel Building Design Code*, Rio de Janeiro, ABNT.

Andrade, S.A.L. Vellasco, P.C.G. Mergulhão, A.J.R. and Lehtola, N. (1995), "A design system used to access the resistance of composite structural members resistant to fire", *Int.Conf. on Education, Practice and Promotion of Comp. Methods in Engineering Using Small Computers - EPMESC V*, Macao, 489-494.

Berner, K. (1988), *Aspects of a New, Fire Resistant Steel/Concrete Composite Construction System*, Internal Report, University of Darmstadt.

Chien, E.Y.L. and Ritchie, J.K. (1984), *Design and Construction of Composite Floor Systems*, Canadian Institute of Steel Construction, CISC.

Jungbluth, O. and Gradwohl, W. (1985), *Berechnen und Bemessen von Verbundprofilstäben Unter Raumtemperatur und für Feuerwiderstandsklassen*, Forschungsbericht Nr. 32/85, Institut für Stahlbau und Werkstoffmechanik, TH Darmstadt.

Jungbluth, O. (1986), *Verbund- und Sandwichtragwerke*, Springer-Verlag, Berlin.

Jungbluth, O. and Gradwohl, W. (1998), *Berechnung und Bemessung von Verbundprofilstäben bei Raumtemperatur und Unter Brandeinwirkung*, Springer-Verlag, Berlin.

Lehtola, N. (1992), "Sistemas estruturais mistos aço/concreto armado resistentes ao fogo", *M.Sc. Dissertation*, Civil Engineering Department, PUC-Rio.

Mergulhão, A.J.R. (1994), "Comportamento de vigas-mistas constituídas por perfis de aço preenchidos com concreto armado", *M.Sc. Dissertation*, Civil Engineering Department, PUC-Rio.

Notation

A_{cr} : Concrete compressive area
A_{rc} : Reinforcing bars compressive area
A_{rt} : Reinforcing bars tension area
A_{sc} : Steel profile compressive area
A_{st} : Steel profile tension area
C : Compressive stress resultant
C_c : Concrete compressive stress resultant
C_r : Reinforcing bars compressive stress resultant
C_s : Steel profile compressive stress resultant
E : Steel elastic modulus
E_c : Concrete elastic modulus
I_r : Transformed reduced composite section moment of inertia with $n=E/2.5E_c$
I_s : Steel profile moment of inertia
I_T : Transformed composite section moment of inertia with $n=E/E_c$
L : Beam span
P : Applied load
T : Tension stress resultant
T_r : Reinforcing bars tension stress resultant
T_s : Steel profile tension stress resultant
W_{LL} : Uniformly distributed live load
W_{LT} : Uniformly distributed long-term live load
W_{SW} : Uniformly distributed self-weight load
a : Distance from the plastic neutral axis to the beam top fibre
f_{cr} : Concrete cylinder strength
f_y : Steel profile yield stress
f_{yr} : Reinforcing bars yield stress
h_c : Distance from the compressive stress resultant to the beam top fibre
h_c' : Distance from the concrete compressive stress resultant to the beam top fibre
h_a' : Lever arm
h_r : Distance from the reinforcing bars tension stress resultant to the beam top fibre
h_r' : Distance from the reinforcing bars compression resultant to the beam top fibre
h_s : Distance from the steel tension stress resultant to the beam top fibre
h_s' : Distance from the steel compression stress resultant to the beam top fibre
h_t : Distance from the tension stress resultant to the beam top fibre
Δ : Total deflection
Δ_{creep} : Creep deflection
Δ_{LL} : Live load deflection
Δ_{shrink} : Shrinkage deflection
Δ_{SW} : Self-weight deflection
ε : Strain
ε_y : Steel strain at yielding onset
γ_{cr} : Concrete density
CC